

TOMOGRAPHIC TESTING OF ALNICO ALLOYS

Damian BAŃKOWSKI, Piotr MŁYNARCZYK, Sławomir SPADŁO, Radosław SÓJKA,
Kamil KLAMCZYŃSKI

Kielce University of Technology, Kielce, Poland, EU, dbankowski@tu.kielce.pl

<https://doi.org/10.37904/metal.2022.4507>

Abstract

We follow an alnico alloy sample to non destructive testing using X-ray radiography. X-ray Computed Tomography (CT), also widely known as MicroCT, is a proven method for not only checking the structural integrity of casting parts - for example for porosity - but also for checking a dimensional accuracy. It is important for assessment casting with complex or small internal areas that could not be inspected by conventional measurements without failure of the final products. Moreover, we were able to visualize the internal defects of the different shapes of casting objects. The gray-value contrasts of the CT images were excellent to distinguish the resin material in the alloy samples. This will be a useful qualitative and quantitative advancement to rapid and detailed non-destructive analysis within the die-casting industries in improving the quality of the alnico alloys.

Keywords: Non destructive testing, X-ray testing, computer topographic testing, alnico alloys

1. INTRODUCTION

Structural integrity of materials is to be monitored to safe operation [1-3]. Regular periodic non-destructive investigation right from the date of installation will not only enable the user to achieve optimum safe utilization but also to alarm when untoward deterioration is caused due to different parameters [4-7]. The estimation of mechanical properties of materials can be carried out by several methods; destructive and non-destructive [8]. By definition, destructive tests lead to permanent damage to the test specimen. It is possible to evaluate the materials - non-destructive tests, which do not destroy the analyzed elements. The non-destructive testing tool, surface and volumetric techniques are used in quality control and quality assessment in all industries [9]. Conventional, non-destructive testing for alloys has been extensively studied, including ultrasonic and radiographic testing [9]. X-ray tomography is a non-destructive method of studying the internal structure of various objects. Radiographic inspection has higher sensitivity, is primarily used to test volume-type defects in casting industries [9]. The principle of operation of a computer tomograph is that the radiation source and detectors move around the object, which is x-rayed with X-rays parallel to the image plane. This radiation passes exactly through the examined object and is attenuated by penetrating through this object [10-12]. The method consists in recording the degree of attenuation of X-rays passing through the tested sample. This weakening depends on the path of the radiation in the material (its thickness) and its absorption capacity [13,14]. The absorption capacity depends on the atomic properties of the substances, thanks to which it is possible to distinguish them in the tested sample. The source of radiation is an x-ray tube, the operating parameters of which, such as power and voltage, are selected depending on the needs. Biological materials - generally with low absorbers - are tested with the use of low-energy radiation. Due to their high absorption capacity, materials such as metals are tested with high-voltage X-ray tubes.

In modern tomographs, the radiation passing through an object is recorded with a semiconductor detector, enabling the observation of the object's interior in real time. In order to be able to represent the three-dimensional internal structure, it is necessary to make multiple projections of the object from different angles.

For this purpose, the source and the detector rotate around the examined object, as in the case of medical tomography, or the object rotates around its axis, and the source-detector system is stationary as in most research and industrial tomographs. The appropriate number of projections (usually several thousand) allows for a precise reconstruction of the internal construction.

In industry, this method is used on an increasing scale. CT is commonly used in defectoscopic examinations and to check the internal structure in the field of materials engineering (e.g. for testing polymers, composites, synthetic materials, ceramics, metals and their alloys), as well as in the electronics industry (e.g. to check the continuity of connections of individual elements), micromechanics (e.g. to check micromechanisms or precise components), geology (e.g. to determine porosity in reservoir rocks, in the study of fossils and minerals), archeology (e.g. in the study of archaeological monuments), biology (e.g. to study the structure of plants and soft and hard biological tissues).

As a result of tomographic examinations it is possible

- analysis of internal defects;
- analysis of the structure of materials;
- nominal-actual comparison with the CAD model;
- analysis of dimensions or wall thicknesses;
- reverse engineering.

Quality assurance and quality control requirements have become increasingly prominent. Therefore testing the internal structure and assessing the integrity of alloys are very important [9]. The visualization and the characterization of the internal architecture of cast Alnico is important to avoid damage during operation. The authors would like to throw some light on this technique of volumetric analysis of alnico alloys.

2. MATERIAL AND EXPERIMENTAL METHODS

Alnico is an acronym referring to the family of ferrous alloys or sinters, which, apart from iron, mainly contain aluminum (Al), nickel (Ni) and cobalt (Co) - hence the name Al-Ni-Co [15]. These alloys sometimes also contain copper and titanium. Alnico alloys are ferromagnetic, with high coercivity (resistance to demagnetization), hence they are used in the production of permanent magnets. The greatest advantage of AlNiCo magnets is high thermal resistance. These magnets can be used up to 525 °C.

The development of alnico alloys began in Japan in 1931, when T. Mishima discovered that an alloy of iron, nickel and aluminum had a coercivity of 32 kA/m, twice as high as the strongest steel magnets at that time [16]. Before the development of magnets containing rare earth elements (eg. neodymium magnets), they were the most powerful of the existing types of magnets [17]. Typical composition of alnico alloys is 8-12 wt% Al, 15-26 wt% Ni, 5-24 wt% Co, up to 6 wt% Cu, up to 1 wt% Ti, supplemented to 100 wt% Fe.

They are used in industrial and consumer applications where a strong permanent magnet is required; examples are electric motors, guitar pickups, microphones, sensors, magnetrons, stomach magnets for cattle [18]. In many applications, they are systematically replaced by stronger rare earth magnets. There are a total of 29 grades of alnico (17 grades of casting alloys, 10 grades sintered, 2 bonded grades). The alloys are under trade names such as Alnico, Columax, Alcomax 3SC, Alni, Hycomax, Ticonal [19]. The composition of Alnico alloy that were investigated is shown in **Table 1**.

Table 1 Chemical composition of the alnico alloy (wt%)

Element	Al	Ti	Fe	Co	Ni	Cu
Average	17.90	0.91	35.16	26.19	15.29	4.56

The volumetric evaluation of Alnico alloys is possible by means of ultrasound or radiographic tests. However, due to the high attenuation of the ultrasonic wave in the case of samples with greater thickness, UT tests are of limited use. The use of the transmission technique (one head sends the other one receives a signal) allows the analysis of larger thicknesses. However, based on the team's research, X-ray examinations are more effective for the 3D evaluation of alnico alloys. The use of appropriate parameters for the execution of a tomographic scan allows for obtaining satisfactory results.

The tomography measurements were carried out at the Laboratory of Radiography and Tomography at the Kielce University of Technology, Poland. The world's first X-ray computed tomography system combining three different radiation sources from Nikon. The laboratory is equipped with:

- two sources of x-ray microfocus 225 kV and 450 kV
- 450 kV minifocus X-ray source.

To ensure stable measurement conditions and to minimize thermal influences during scans of long duration laboratory is equipped with air and liquid cooling system. X-ray was used for converting images. The reconstructed data were processed and visualized with the software VG Studio 3.4.1. Segmentation was performed using global grey -value thresholds [14]. Castings tend to form shrinkage cavities due to the reduction in metal volume during cooling and solidification. In addition, we can distinguish scars, blisters, tears, scabs, cracks [20-25]. In the case of the analyzed Alnico alloy, the most frequently observed foundry imperfections are pores, micropores, blisters and cracks.

As a result of the tests carried out with the use of X-rays, it was possible to visualize internal defects [26]. **Figure 1** shows a 3D reconstruction of a disc with a diameter of 40 mm and a height of 20 mm. As a result of ultrasonic tests, the defect was revealed at a depth of about 9.5 mm. On the basis of **Figure 2** and the analysis of the tomographic reconstruction allowed for precise dimensioning of the defect along with its location. From the point of view of the defect assessment, the most important thing is its length, which was 9.2588 mm and the void volume was 10.99 mm³. The verification of the placement confirmed that the void is at a depth of 9.2588 mm.

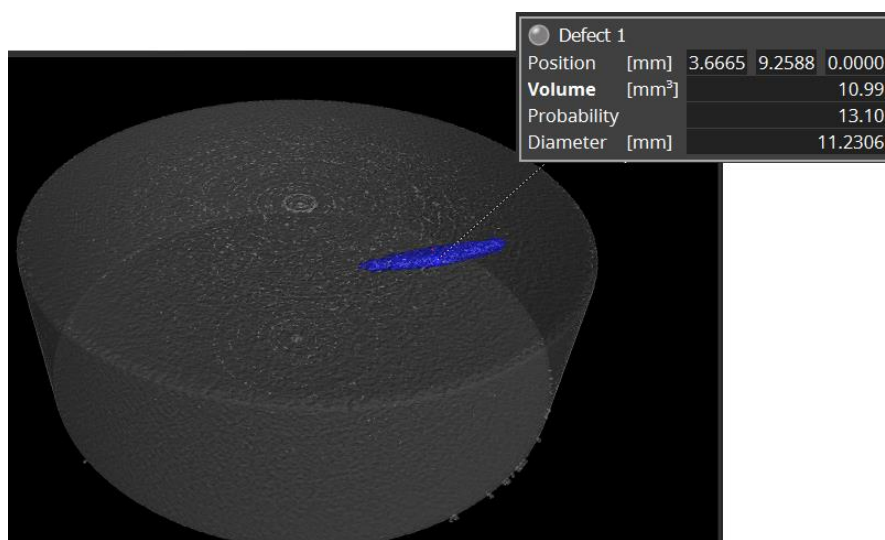


Figure 1 3D tomographic reconstruction of the cylindrical alnico alloy casting with the void area marked in blue and the defect features (volume, location)

Figure 2 shows a 3D tomographic reconstruction of a ring with an outer diameter of 50 mm and an inner diameter of 30 mm. The colours represent the volumes of the individual defects. Blue indicates defects with a volume below 1 mm³, and red indicates defects larger than 6 mm³.

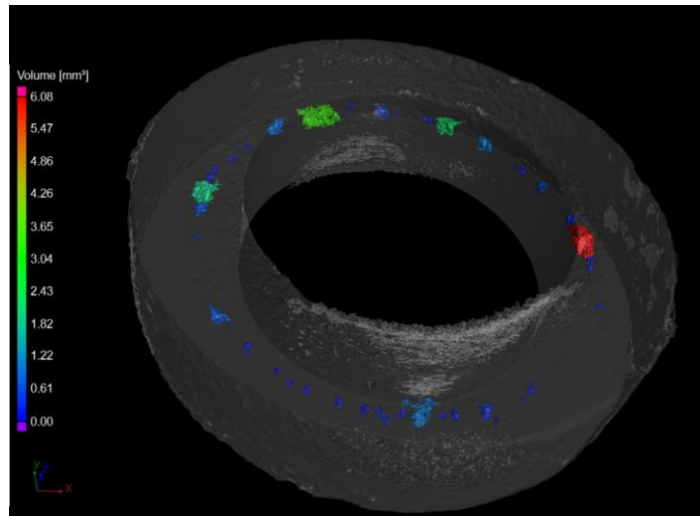


Figure 2 3D tomographic reconstruction of the alnico ring with the defects marked

Figure 3 shows a view of three sections of the 3D model and the model itself. As a result of setting the transparency at the level of 80%, it is possible to observe internal defects in the 3D model.

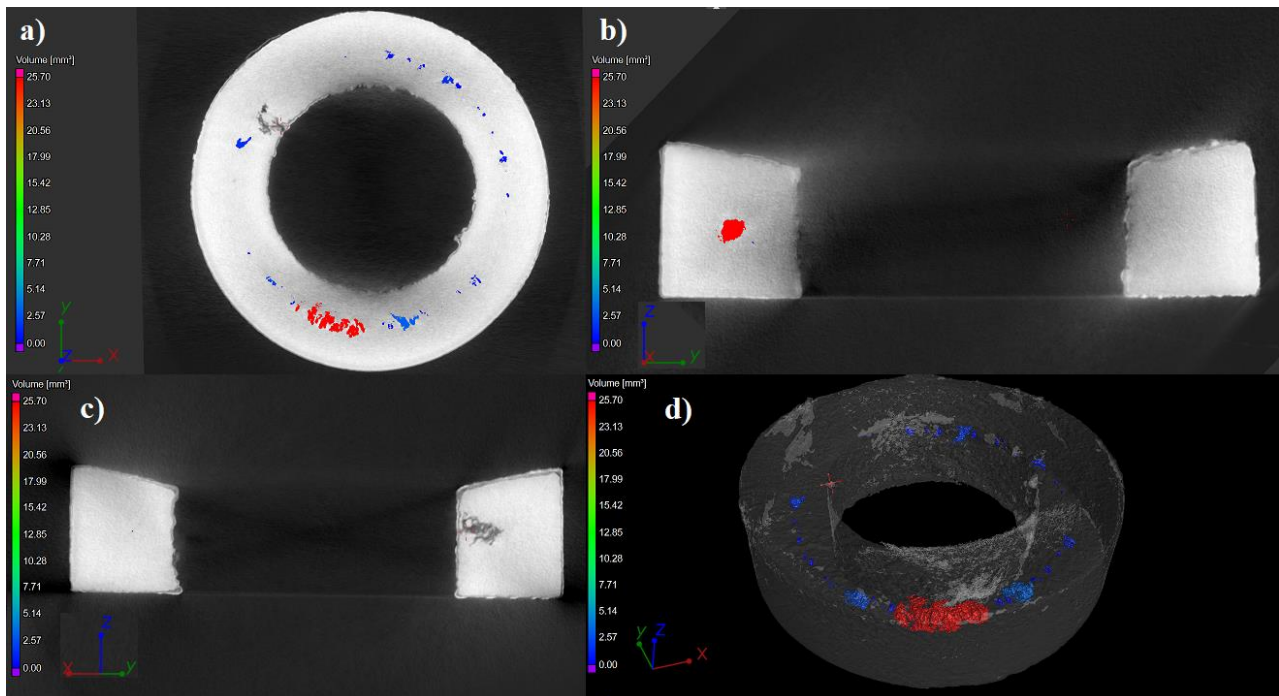


Figure 3 Screen view from VG Studio showing cross sections with the defects marked a) x-y section; b) z-y section; c) x-z section; d) 3D model

By analyzing the cross-sections in individual axes, it can be stated that the defects are centrally located. It is especially visible along the Z axis, between the top and bottom - **Figure 3 b**). The occurrence of air bubbles, air voids, gases may indicate significant gassing of the casting. As a result of the crystallization and solidification of the metal, the volume of the casting is reduced and, as a consequence, there are voids in the casting. Measurements of the distance between the location of most internal defects prove that the casting is cooled evenly towards the top and bottom walls. However, as in **Figure 3 c**), a greater density of defects can be noticed near the inner radius - the hole in the analyzed ring. This may prove a lower cooling speed of

internal walls than in the vicinity of external walls. Research confirms the occurrence of large bladder defects with a volume of up to 25 mm³, which are unacceptable. This may be a defect in the form of voids, blisters due to clotting. The analysis of a larger number of samples proves that there are Alnico alloy rings without internal defects and these samples containing incompatibilities can be distinguished.

In addition, specialized software allows you to summarize all indications (defects) in the form of a sheet containing all information about each of the specified internal non-conformities. As an example, **Table 2** shows inconsistencies with their characteristics for the defect radius greater than 1 mm condition.

Table 2 Data for a selected sample made of alnico alloy with details of dimensions and location of defects

Radius (mm)	Diameter (mm)	Volume (mm ³)	Surface (mm ²)	Projected size x (mm)	Projected size y (mm)	Projected size z (mm)
7.2218	14.4436	25.08	723.4	14.3087	9.0072	6.794
4.6506	9.3013	3.6	52.95	3.1911	7.9264	7.1543
3.2412	6.4825	7.31	103.93	5.2499	4.9926	3.2426
2.2921	4.5842	3.9	67.11	4.3235	3.397	3.2426
2.2392	4.4784	0.92	20.65	4.2205	2.625	1.8014
1.9309	3.8618	1.22	14.8	1.75	2.7794	3.1397
1,6123	3.2247	1.28	15.37	2.8823	1.9559	2.2647
1.4338	2.8676	0.96	16.25	2.1617	2.2647	1.9044
1.2676	2.5353	0.85	17.23	2.3676	2.1103	2.0073
1.1781	2.3562	0.24	4.58	1.9559	1.4412	1.0809
1.0853	2.1706	0.33	5.83	1.0294	1.8014	1.5441

The VG Studio software also enables verification and comparison of the performed tomographic reconstruction with the CAD geometry design. As can be seen in **Figure 4**, the colours in the model on the right show the deviations from the reference geometry. It is also possible to verify that the raw casting after machining will not contain defects on the surface (side walls). **Figure 4 a)** shows the adjustment of the CAD model (dark gray) to the actual sample - cast - marked with light gray. There is a mismatch probably resulting from an error in the casting mold. **Figure 4b)** shows the matching of the CAD model with the final real object. Blue and purple indicate negative deviations, while yellow and red are positive deviations. A negative deviation informs about the lack of material, and a positive deviation informs about the need to remove excess material.

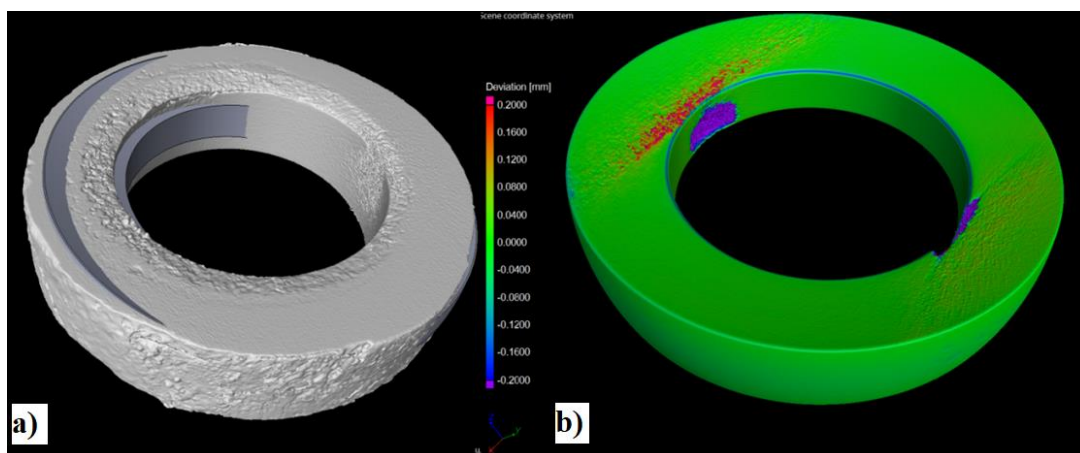


Figure 4 Verification of a tomographic scan with a CAD model

3. CONCLUSION

Tomographic examinations make it possible to identify almost all existing defects in the tested alnico detail.

With the help of tomographic examinations, it is possible to locate non-compliance in the volume of the X-rayed materials.

The use of appropriate exposure conditions, i.e. distance lamp, scanned object - scanned object - detector, type and thickness of the diaphragm allows for clear reconstructions of alnico alloys.

The use of shutters reduces image blur caused by stray radiation.

About half of the tested Alnico castings have symmetrically arranged internal voids, gas bubbles formed during solidification.

ACKNOWLEDGEMENTS

The research reported herein was supported by a grant from the National Centre for Research and Development. Program: Lider XI, grant title: "Improvements in the technology of machining the surfaces of spherical rings of magneto mirrors through the use of electro-erosion machining (EDM)", contract number: LIDER/59/0246/L-11/19/NCBR/2020

REFERENCES

- [1] BAŃKOWSKI, D., MŁYNARCZYK, P. Visual Testing of Castings Defects after Vibratory Machining. *Archives of Foundry Engineering*. 2020, vol. 4, pp. 72-76.
- [2] BANKOWSKI, D., SPADLO, S. Investigations of influence of vibration smoothing conditions of geometrical structure on machined surfaces. In *4th International Conference Recent Trends in Structural Materials*. 2016, vol. 179, Article Number: UNSP 012002. Available from: <https://doi.org/10.1088/1757-899X/179/1/012002>.
- [3] BAŃKOWSKI, D. SPADLO, S. Influence of the smoothing conditions in vibro-abrasive for technically dry friction the parts made of steel X160CrMoV121. In: *Proceedings of 25th International Conference on Metallurgy and Materials. Metal 2016*. 2016, pp. 1019-1024.
- [4] SPADŁO, S., BAŃKOWSKI, D., MŁYNARCZYK, P., HLAVÁČOVÁ, I.M. Influence of local temperature changes on the material microstructure in abrasive water jet machining (AWJM). *Materials*. 2021, vol. 14, no. 18.
- [5] MILLER, T., ADAMCZAK, S., ŚWIDERSKI, J., WIECZOROWSKI, M., ŁĘTOCHA, A., GAPIŃSKI, B. Influence of temperature gradient on surface texture measurements with the use of profilometry. *Bulletin of the Polish Academy of Sciences-Technical Sciences*. 2017, vol. 65, no. 1, pp. 53-61.
- [6] CHEN, S. MA, S. CHEN, Z. YUE, X., CHANG, G. Casting defects in transition layer of Cu/Al composite castings prepared using pouring aluminum method and their formation mechanism. *High Temperature Materials and Processes*. 2019, vol. 38, pp. 199-206.
- [7] ŚWIŁŁO, S.J., PERZYK, M. Surface casting defects inspection using vision system and neural network techniques. *Archives of Foundry Engineering*. 2013, vol. 13, issue 4, pp. 103-106.
- [8] CHOKKALINGAM, B., RAJA, V., ANBURAJ, J., IMMANUAL, R., DHINESHKUMAR, M. Investigation of shrinkage defect in castings by quantitative Ishikawa diagram. *Archives of Foundry Engineering*. 2017, vol. 17, Issue: 1, pp. 174-178.
- [9] ŚWIŁŁO, S.J., MYSZKA, D. Advanced metrology of surface defects measurement for aluminum die casting. *Archives of Foundry Engineering*. 2011, vol. 11, Issue: 3, pp. 227-230.
- [10] NANDAGOPAL, M., SIVAKUMAR, K., SENGOTTUVELAN, M., VELMURUGAN, S. Review on ferrous and non-ferrous casting defects and their analysis. *AIP Conference Proceedings*, 2128. 030010. 2019. Available from: <https://doi.org/10.1063/1.5117953>.
- [11] MEROLA, M., CHAPPUIS, P., ESCOURBIAC, F., GRATAROLA, M., JESKANEN, H., KAUPPINEN, P., PLÖCHL, L., SCHEDLER, B., SCHLOSSER, J., SMID, I., TÄHTINEN, S., VESPRINI, R., VISCA, E., ZABERNIG, A. Non-destructive testing of divertor components. *Fusion Engineering and Design*. 2002, vol. 61-62, pp. 141-146.

- [12] KASHYAP, SK., LAXMINARAYNA, G., TEWARI, S., SINHA, A. Non-destructive testing of steel wire ropes and their discard criteria. In: *8th International Conference of the Slovenian Society for Non-Destructive Testing*. 2005, Conference Proceedings, Book Subtitle. Application of Contemporary Non-Destructive Testing in Engineering. pp. 229-235.
- [13] MALEK, J., MACHTA K. Destructive and non-destructive testing of concrete structures. *Jordan Journal of Civil Engineering*. 2014, pp. 432-441.
- [14] BO, H., RUNQIAO, Y., HENGCAI, Z. Magnetic non-destructive testing method for thin-plate aluminum alloys. *NDT & E International*. 2012, vol. 47, pp. 66-69.
- [15] RAJA, A.Y., MOGHISEH, M., BATEMAN, C.J., DE RUITER, N., SCHON, B., SCHLEICH, N., WOODFIELD, T.B.F., BUTLER, A.P.H., ANDERSON, N.G. Measuring identification and quantification errors in spectral CT material decomposition. *Appl. Sci*. 2018, vol. 8, p. 467. Available from: <https://doi.org/10.3390/app8030467>.
- [16] LEE W. Principles of CT: Multislice CT. Goldman. *Journal of Nuclear Medicine Technology*. June 2008, vol. 36. no. 2, pp. 57-68. Available from: <https://doi.org/10.2967/jnmt.107.044826>.
- [17] LANBO L., TIESHUAN G. Seismic non-destructive testing on a reinforced concrete bridge column using tomographic imaging techniques. *Journal of Geophysics and Engineering*. 2005, vol. 2, issue 1, pp. 23-31. Available from: <https://doi.org/10.1088/1742-2132/2/1/004>.
- [18] MAROUFIAN S. S., PILLAY P. Design and analysis of a novel PM-assisted synchronous reluctance machine topology with AlNiCo magnets. *IEEE Transactions on Industry Applications*. 2019, vol. 55, no. 5, pp. 4733-4742. Available from: <https://doi.org/10.1109/TIA.2019.2925784>.
- [19] <https://pl.wikipedia.org/wiki/Alnico> (2022-04-22).
- [20] CULLITY B. D., GRAHAM C. D. *Introduction to Magnetic Materials*. 2008, vol. 2. Wiley, pp. 485. ISBN 978-0-471-47741-9.
- [21] e-Magnets UK: *Alnico Magnets: An Introduction to Alnico Magnets* (ang.). [2014-09-07].
- [22] BANKOWSKI, D., SPADLO, S. The use of abrasive waterjet cutting to remove flash from castings. *Archives of Foundry Engineering*. 2019, vol. 19, issue: 3, pp. 94-98.
- [23] ASGHAR, Z., REQUENA, G., SKET, F. Multiscale tomographic analysis of heterogeneous cast Al-Si-X alloys. *Journal of Microscopy*. 2015, vol. 259, issue 1, pp. 1-9.
- [24] SWIERCZ, R. ONISZCZUK-SWIERCZ, D. DABROWSKI, L. Electrical discharge machining of difficult to cut materials. *Archive of Mechanical Engineering*. 2018, vol. 65, issue: 4, pp. 461-476. Available from: <https://doi.org/10.24425/ame.2018.125437>.
- [25] ONISZCZUK-SWIERCZ, D., SWIERCZ, R. Surface texture after wire electrical discharge machining. In: *Proceedings of 26th International Conference on Metallurgy and Materials*. 2017, pp. 1400-1405.
- [26] PAESANO A., FERREIRA, R. F., SCHAFER, D., ALVES, T. J. B., FORTUNATO, J., IVASHITA, F. F. Application of the modified Rayleigh model in the mathematical analysis of Alnico II minor loops. *Physics of Condensed Matter*. 2021, vol. 612, no. 12, pp. 1-4. Available from: <https://doi.org/10.1016/j.physb.2020.412629>.